ARTICLE

Pharmacologic conversion of cancer-associated fibroblasts from a protumor phenotype to an antitumor phenotype improves the sensitivity of pancreatic cancer to chemotherapeutics

Tadashi Iida[1,2,12], Yasuyuki Mizutani[1,2,12], Nobutoshi Esaki[1], Suzanne M. Ponik[3], Brian M. Burkel[3], Liang Weng[4], Keiko Kuwata[5], Atsushi Masamune[6], Seiichiro Ishihara[7], Hisashi Haga[7], Kunio Kataoka[1,2], Shinji Mii[1], Yukihiro Shiraki[1], Takuya Ishikawa[2], Eizaburo Ohno[2], Hiroki Kawashima[2,8], Yoshiki Hirooka[9], Mitsuhiro Fujishiro[2,11], Masahide Takahashi[10] and Atsushi Enomoto[1]✉

Previous therapeutic attempts to deplete cancer-associated fibroblasts (CAFs) or inhibit their proliferation in pancreatic ductal adenocarcinoma (PDAC) were not successful in mice or patients. Thus, CAFs may be tumor suppressive or heterogeneous, with distinct cancer-restraining and -promoting CAFs (rCAFs and pCAFs, respectively). Here, we showed that induced expression of the glycosylphosphatidylinositol-anchored protein Meflin, a rCAF-specific marker, in CAFs by genetic and pharmacological approaches improved the chemosensitivity of mouse PDAC. A chemical library screen identified Am80, a synthetic, nonnatural retinoid, as a reagent that effectively induced Meflin expression in CAFs. Am80 administration improved the sensitivity of PDAC to chemotherapeutics, accompanied by increases in tumor vessel area and intratumoral drug delivery. Mechanistically, Meflin was involved in the suppression of tissue stiffening by interacting with lysyl oxidase to inhibit its collagen crosslinking activity. These data suggested that modulation of CAF heterogeneity may represent a strategy for PDAC treatment.

Graphical Abstract
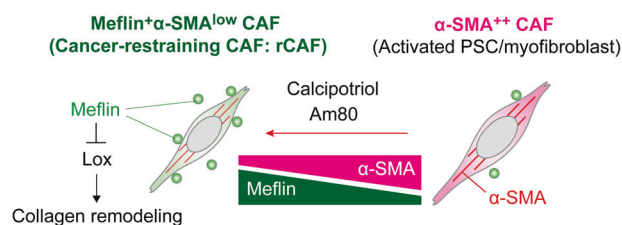
INTRODUCTION

A well-known feature of pancreatic ductal adenocarcinoma (PDAC) is the proliferation of cancer-associated fibroblasts (CAFs), excessive deposition of the extracellular matrix (ECM) proteins produced by CAFs, and ECM remodeling in the stroma [1]. CAF proliferation and ECM deposition are also found in many other recalcitrant cancers and constitute a major compartment of the tumor microenvironment (TME) along with tumor vessels and immune cells [2–7]. CAFs promote cancer progression through various mechanisms and secrete various soluble factors, including growth factors, chemokines and cytokines, insoluble ECM, proteases, and extracellular vesicles, which may promote the

[1]Department of Pathology, Nagoya University Graduate School of Medicine, Nagoya, Japan. [2]Department of Gastroenterology and Hepatology, Nagoya University Graduate School of Medicine, Nagoya, Japan. [3]Department of Cell and Regenerative Biology, University of Wisconsin-Madison, Madison, WI, USA. [4]Department of Oncology, Xiangya Cancer Center, Xiangya Hospital, Central South University, Changsha, China. [5]Institute of Transformative Bio-Molecules, Nagoya University, Nagoya, Japan. [6]Division of Gastroenterology, Tohoku University Graduate School of Medicine, Sendai, Japan. [7]Faculty of Advanced Life Science, Hokkaido University, Sapporo, Japan. [8]Department of Endoscopy, Nagoya University Hospital, Nagoya, Japan. [9]Department of Gastroenterology and Hepatology, Fujita Health University, Toyoake, Aichi, Japan. [10]International Center for Cell and Gene Therapy, Fujita Health University, Toyoake, Japan. [11]Present address: Department of Gastroenterology, Graduate School of Medicine, The University of Tokyo, Tokyo, Japan. [12]These authors contributed equally: Tadashi Iida, Yasuyuki Mizutani. ✉email: enomoto@iar.nagoya-u.ac.jp

Table 1. Characteristics of patients with PDAC included in the current study.

Characteristics		Total	Meflin high	Meflin low	χ^2 test *P* value
Number		33	10	23	
Median age (years)		68	65	68	
Sex	Male	23	8	15	0.3958
	Female	10	2	8	
TNM stage	T3N0M1	7	1	6	
	T3N1M1	5	2	3	
	T4N0M0	6	3	3	
	T4N1M0	3	1	2	
	T4N0M1	10	2	8	
	T4N1M1	2	1	1	
Clinical stage	III	10	4	6	0.4241
	IV	23	6	17	
Chemotherapy	FOLFILINOX	7	3	4	0.4217
	GnP and Gem (Gem)	26	7 (2)	19 (2)	

proliferation, invasion, and metastasis of cancer cells and contribute to drug resistance and suppression of antitumor immunity [2–9]. These findings have facilitated recent efforts to develop therapeutics that deplete CAFs or inhibit their proliferation and functions [2, 5–7, 10–12].

CAFs were previously thought to be a uniform population of cells with cancer-promoting functions. However, several preclinical and clinical attempts to target CAFs in PDAC mouse models and patients were not therapeutically successful, and some intervention strategies resulted in disease progression [3, 10, 11]. Thus, certain subtype(s) of CAFs may suppress rather than support the progression of PDAC [2, 5–7]. Recent studies showed that the antitumor activity of collagen type I produced by CAFs could shape the immune microenvironment and suppress PDAC progression [13, 14]. By contrast, distinct subsets of CAFs with cancer-promoting and cancer-restraining functions may exist [2, 5–7]. Indeed, recent single-cell transcriptomic analyses have shown that CAFs can be classified into many subsets [15, 16]. The most relevant and characterized CAF subsets in PDAC are myofibroblastic CAFs (myCAFs), inflammatory CAFs (iCAFs), and antigen-presenting CAFs [16, 17]. Clinicopathological and pharmacological studies have shown that these CAFs exert protumor effects through diverse mechanisms [15, 18, 19]. However, the existence of cancer-restraining CAFs (rCAFs) and their marker proteins has not been investigated.

We recently identified the new CAF marker Meflin, a glycosylphosphatidylinositol (GPI)-anchored membrane protein encoded by the immunoglobulin superfamily containing leucine-rich repeat (*Islr*) gene, in both mouse and human PDAC [7, 20–22]. Single-cell analyses of CAFs of mouse PDAC showed that Meflin marks a subset of CAFs distinct from α-smooth muscle actin (SMA)$^+$ myCAFs and interleukin (IL)-6$^+$ iCAFs [15, 17, 20]. Furthermore, our analyses of human PDAC samples, an autochthonous PDAC mouse model, tumor transplantation models, and cell biological assays showed that Meflin suppresses PDAC progression, suggesting that Meflin is a marker of rCAFs [7, 20]. Interestingly, a lineage tracing experiment showed that Meflin$^+$ rCAFs, which appear in the very early stages of cancer, give rise to α-SMA$^+$ CAFs that are negative or weakly positive for Meflin during cancer progression, suggesting that Meflin$^+$ rCAFs differentiate into other CAF types, including myCAFs and iCAFs [7, 20, 22]. Moreover, induction of Meflin expression in Meflin$^-$ CAFs blocks PDAC progression in a tumor transplantation model, indicating that CAF function is determined by the net balance of the expression of cancer-promoting and—restraining proteins [20]. In norma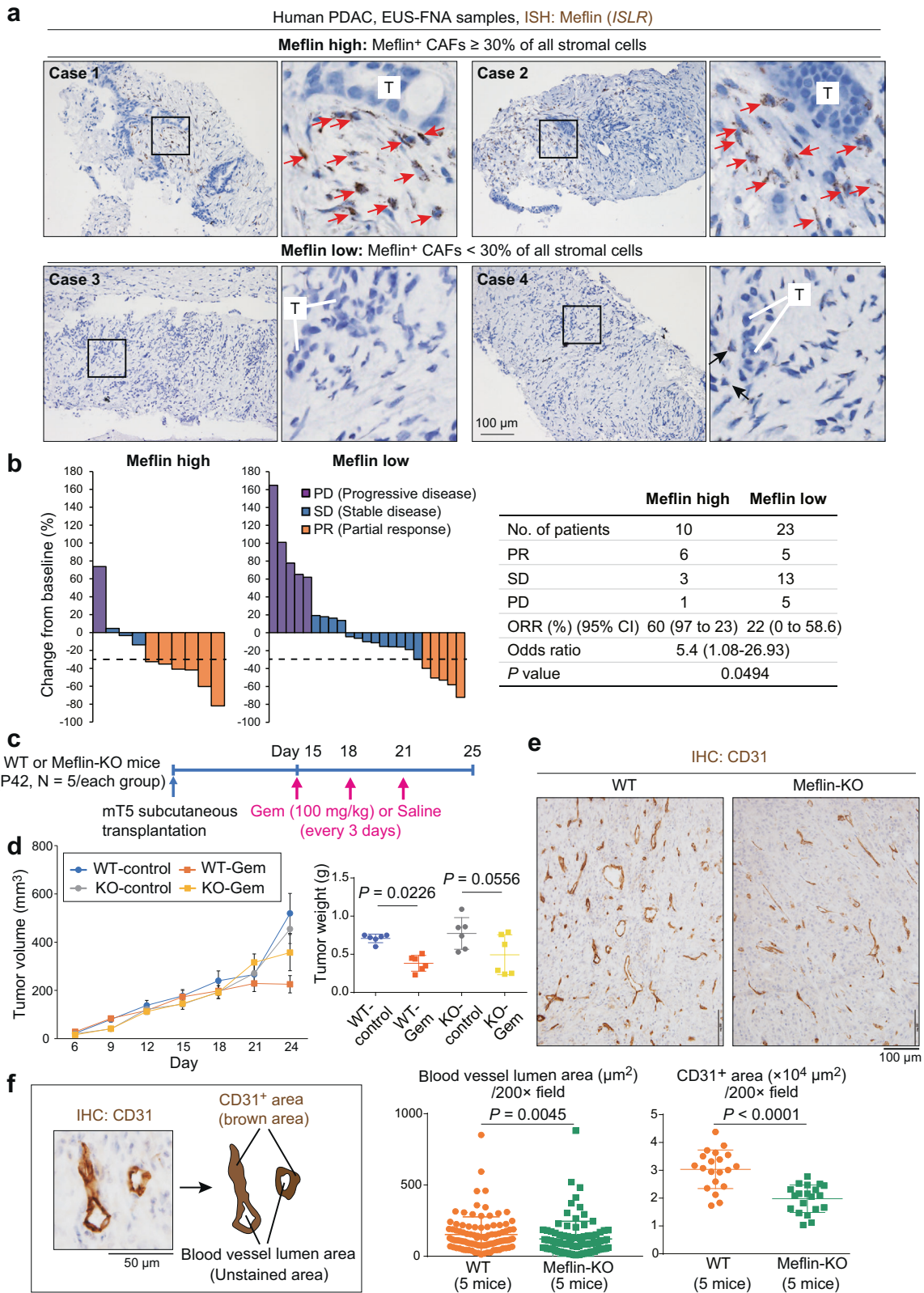l tissues, Meflin is expressed by pancreatic stellate cells (PSCs) in the pancreas and mesenchymal stem cells (MSCs) in the bone marrow and most other tissues, both of which are known to be major origins of CAF [20–26]. Therefore, rCAFs may be proliferating naïve (undifferentiated) PSCs or MSCs, which, as the tumor progresses, differentiate into Meflin-negative or -weakly positive cancer-promoting CAFs (pCAFs) [7, 20].

Given that Meflin is a functional marker of rCAFs in PDAC, one plausible strategy to treat PDAC may be to selectively induce Meflin expression in CAFs to change their phenotype. Accordingly, in this study, we first used a recombinant Sendai virus (SeV) vector to deliver the *Islr* gene, which encodes Meflin, to CAFs in a tumor transplantation mouse model. We then screened a chemical library and identified the synthetic unnatural retinoid Am80 as a compound that significantly induced Meflin expression in CAFs. Oral administration of Am80 to a PDAC transplantation mouse model significantly upregulated Meflin expression in CAFs and improved the sensitivity of tumors to conventional chemotherapeutics. We also provided mechanistic insights into the roles of Meflin in shaping the cancer-restraining TME. These findings suggest that the modulation or manipulation of CAF phenotypes by genetic or pharmacological intervention may represent a practical strategy for PDAC treatment.

RESULTS
Meflin expression in CAFs correlated with better responses to chemotherapeutics in human PDAC
Our previous study showed that the number of Meflin$^+$ CAFs is correlated with favorable clinical outcomes in patients with stage II and III borderline resectable and locally advanced PDAC [20]. Here, we examined the expression of Meflin in CAFs in biopsy samples obtained from patients with PDAC who underwent chemotherapy (gemcitabine [Gem] alone, Gem plus nab-paclitaxel [nabPTX; GnP]), or FOLFIRINOX) at our institution (Table 1) and evaluated correlations with objective response rates (ORRs; Fig. 1a, b). As previously reported [20], in situ hybridization (ISH) analysis showed that Meflin expression was specifically observed in fibroblastic cells in the stroma, which represent CAFs, but not in other cell types, such as epithelial (tumor), endothelial, smooth muscle, immune, and blood cells, in PDAC tissues (Fig. 1a). Cases in which at least 30% of stromal cells were positive for Meflin were classified as Meflin high, whereas other cases were classified as Meflin low. Interestingly, some but not all CAFs expressed Meflin, and Meflin positivity in all CAFs was correlated with higher ORRs (Fig. 1b). Thus, we hypothesized that Meflin$^+$ CAFs may enhance the chemosensitivity of PDAC.

a

Human PDAC, EUS-FNA samples, ISH: Meflin (*ISLR*)

Meflin high: Meflin+ CAFs ≥ 30% of all stromal cells

Meflin low: Meflin+ CAFs < 30% of all stromal cells

b

	Meflin high	Meflin low
No. of patients	10	23
PR	6	5
SD	3	13
PD	1	5
ORR (%) (95% CI)	60 (97 to 23)	22 (0 to 58.6)
Odds ratio	5.4 (1.08-26.93)	
P value	0.0494	

c

d

e

IHC: CD31

f

This hypothesis was further supported by experiments in a tumor transplantation mouse model. We subcutaneously implanted mT5 cells, a mouse PDAC cell line [27], into WT and Meflin-KO mice [21], followed by treatment with Gem (Fig. 1c). ISH analysis detected Meflin mRNA specifically in stromal cells in tumors developed in WT but not Meflin-KO mice, supporting the notion that Meflin is a marker of CAFs in mouse tumors (Supplementary Fig. 1). Notably, Gem treatment significantly reduced the volume of the implanted tumors in WT mice but not Meflin-KO mice, demonstrating the importance of Meflin

Fig. 1 Numbers of Meflin$^+$ stromal cells correlated with response of patients with PDAC to chemotherapeutics and tumor vessel area.
a Representative images of Meflin ISH analysis on formalin-fixed and paraffin-embedded (FFPE) sections of biopsy samples obtained from patients with PDAC by endoscopic ultrasound-guided fine needle aspiration (EUS-FNA). Cases with 30% or more of stromal cells positive for Meflin were classified as Meflin high (cases 1 and 2, upper panel), whereas others were classified as Meflin low (cases 3 and 4, lower panel). Boxed areas were magnified in adjacent panels. Red arrows indicate Meflin$^+$ CAFs. Black arrows indicate CAFs weakly positive for Meflin. T tumor cells. **b** Waterfall plots depicting tumor responses of patients with PDAC ($N = 33$), who received Gem, nabPTX plus Gem (GnP), or FOLFIRINOX, evaluated by the Response Evaluation Criteria in Solid Tumors (RECIST) criteria. The table in the right panel shows the numbers of patients classified by their response status and Meflin expression. The results of statistical analysis are also shown. **c** WT and Meflin-KO female mice at postnatal day (P) 42 were subcutaneously transplanted with mT5 mouse PDAC cells (1×10^6 cells/mouse), followed by i.p. administration of Gem or saline three times every 2 days and sacrifice at day 25. **d** Time course of the volumes of tumors developed in WT and Meflin-KO mice administered saline or Gem (left panel) and quantification of tumor weight at the end of the experiment (right panel). **e** Representative images of tissue sections of WT and Meflin-KO mT5 tumors stained for CD31. Brown color denotes positivity. IHC immunohistochemistry. **f** Schematic illustration depicting the method of quantification of CD31-stained blood vessel area and lumen of mT5 tumors in WT and Meflin-KO mice, performed using ImageJ software (left panel). Quantification data are shown in middle and right panels.

expression in CAFs in tumor chemosensitivity (Fig. 1d). Consistent with our previous report showing that Meflin-KO mice developed PDAC with decreased tumor vessel areas when crossed with the Kras$^{LSL-G12D/+}$; Trp53$^{LSL-R172H/+}$; Pdx-1-Cre (KPC) autochthonous PDAC model [20, 28], mT5 tumors implanted into Meflin-KO mice exhibited decreases in the lumen of tumor vessel and CD31$^+$ endothelial areas compared with WT mice (Fig. 1e, f). Thus, Meflin expression in CAFs was associated with chemosensitivity and tumor vessel perfusion, in contrast to the prevailing notion that most CAFs contribute to chemoresistance [29, 30].

SeV-mediated Meflin expression improved PDAC sensitivity to Gem

To induce Meflin expression in CAFs, we generated a SeV encoding mouse Meflin (Supplementary Fig. 2a, b). Infection of primary cultured mouse MSCs with SeV-Meflin (3×10^7 cell infectious units [CIU]) resulted in a significant increase in Meflin expression compared with a control SeV vector encoding DasherGFP (DGFP; Fig. 2a). This was accompanied by the downregulation of myCAF and iCAF markers, such as α-SMA (*Acta2*), collagen type I and III (*Col1a1 and Col3a1*), and IL-6 (*Il6*; Fig. 2b, Supplementary Fig. 2c). The effects of SeV-mediated Meflin expression on CAF markers, except collagen types I and III, were also confirmed in the MSC line C3H10T1/2 (Supplementary Fig. 2d). Next, we found that injection of SeV-Meflin into subcutaneous mT5 tumors in WT mice induced Meflin overexpression and decreased α-SMA expression and collagen deposition (Fig. 2c, d, Supplementary Fig. 3a). Contrary to our initial expectations, we did not observe any effects of repeated transduction of SeV-Meflin on tumor progression (Fig. 2e, f). However, mT5 tumors transduced with SeV-Meflin exhibited a significant increase in tumor vessel area (Fig. 2g, h) and sensitivity to Gem treatment (Fig. 2i, j). The proliferation rates of mT5 and C3H10T1/2 cells infected with SeV-Meflin and their sensitivity to Gem were comparable to those of control cells in culture (Supplementary Fig. 4). Notably, SeVs infected stromal fibroblastic cells but not endothelial cells and pericytes present in the tumors (Supplementary Fig. 5). These data suggested that induction of Meflin expression in tumors enhanced their sensitivity to Gem through changes in the stromal compartment but not tumor cells. The effects of SeV-Meflin on collagen deposition, but not α-SMA expression in CAFs, persisted even after Gem treatment, suggesting a strong regulatory role of Meflin in collagen homeostasis (Supplementary Fig. 3b).

Interestingly, we observed a rescue effect of SeV-mediated Meflin transduction on the progression of mT5 tumors developed in Meflin-KO mice (Supplementary Fig. 6). Induction of Meflin expression by SeV-Meflin significantly suppressed mT5 tumor growth in Meflin-KO mice, but not in WT mice (Supplementary Fig. 6a, b). ISH analysis showed that α-SMA expression in the tumor stroma was downregulated by Meflin expression in tumors in Meflin-KO mice (Supplementary Fig. 6c). These data supported that Meflin may suppress α-SMA expression in CAFs and thereby block cancer progression.

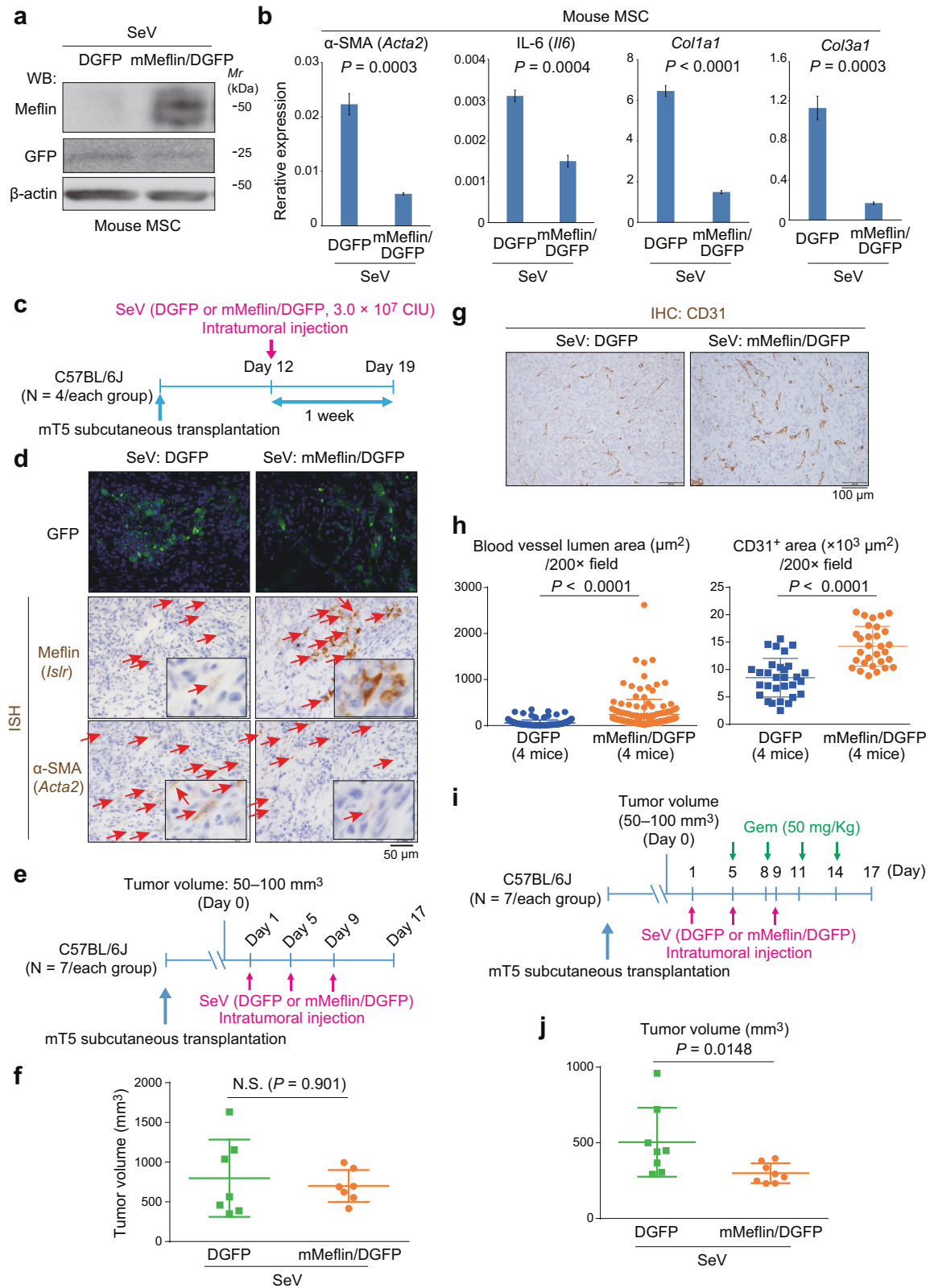### Identification of Am80 as an inducer of Meflin expression in CAFs

The findings described above suggested that programming CAFs to overexpress Meflin or convert Meflin$^{-/low}$ CAFs to Meflin$^+$ rCAFs may improve the chemosensitivity of PDAC. Moreover, administration of calcipotriol, a vitamin D analogue, to PDAC model mice improves tumor sensitivity to Gem [31], and all-trans-retinoic acid (ATRA) reprograms activated PSCs to inhibit tumor progression through suppression of ECM remodeling [32]. These studies have been the basis of ongoing clinical trials evaluating the efficacy of combination therapies of vitamin D analogues, ATRA, and conventional chemotherapeutics in patients with advanced PDAC (https://clinicaltrials.gov/) [33]. We previously showed that calcipotriol treatment upregulated Meflin in PDAC CAFs [20], suggesting that Meflin expression may mediate the effects of calcipotriol and ATRA on improving outcomes in patients with PDAC. Accordingly, in this study, we screened a library of nuclear receptor ligands to identify compounds that effectively upregulate Meflin expression in CAFs using human PSCs isolated from pancreatic tissues adjacent to PDAC and cultured long-term on plastic, which exhibit essentially the same properties as CAFs [31], and mouse MSCs, which are a known CAF origin in mice (Supplementary Fig. 7a, b). Among the compounds that upregulated Meflin in both cell types, we identified Am580, a synthetic retinoid and retinoic acid receptor (RAR) α-selective agonist [34, 35].

We next validated the effects of Am580 and another synthetic retinoid Am80, which is a retinobenzoic acid that is structurally related to Am580 [34, 35], on the expression of Meflin and other CAF marker genes in mouse MSCs (Fig. 3a). Am580, Am80, and ATRA upregulated Meflin and downregulated α-SMA, collagen type I and III, and IL-6, suggesting potential applications in conversion of the CAF phenotype. Because Am80 is approved for treating patients with recurrent and intractable acute promyelocytic leukemia (APL) in Japan (trade name: Tamibarotene) [36], we next explored the in vivo effects of Am80 in PDAC progression in further experiments.

Oral administration of varying doses of Am80 to WT mice harboring subcutaneous mT5 tumors affected neither body weight nor tumor volume and weight (Fig. 3b–e). Am80 at a very high concentration (10 μM) inhibited the proliferation of cultured mT5 cells, but did not affect mT5 proliferation when used at concentrations ranging from 0.01 to 1 μM (Supplementary Fig. 8). ISH analysis of mT5 tumor tissues showed that Meflin expression in stromal cells was highly upregulated by Am80 administration, accompanied by downregulation of α-SMA and collagen deposition (Fig. 3f, Supplementary Fig. 9a). As expected from analyses of human PDAC biopsy samples and mT5 tumors transduced with SeV-Meflin (Figs. 1, 2), Am80 administration increased tumor vessel area in the mT5 tumor transplantation model (Fig. 3g).

Am80 administration enhanced the effects of chemotherapeutics

We next orally administered Am80 to WT mice harboring mT5 tumors for 1 week, followed by treatment with Am80 plus Gem

a

SeV

WB: DGFP mMeflin/DGFP

Meflin

GFP

β-actin

Mouse MSC

b Mouse MSC

α-SMA (*Acta2*)   IL-6 (*Il6*)   *Col1a1*   *Col3a1*

$P = 0.0003$ $P = 0.0004$ $P < 0.0001$ $P = 0.0003$

c

SeV (DGFP or mMeflin/DGFP, 3.0×10^7 CIU)
Intratumoral injection

C57BL/6J (N = 4/each group)

Day 12   Day 19

1 week

mT5 subcutaneous transplantation

d

SeV: DGFP   SeV: mMeflin/DGFP

GFP

ISH — Meflin (*Islr*), α-SMA (*Acta2*)

50 μm

e

Tumor volume: 50–100 mm^3 (Day 0)

C57BL/6J (N = 7/each group)

Day 1 Day 5 Day 9   Day 17

SeV (DGFP or mMeflin/DGFP)
Intratumoral injection

mT5 subcutaneous transplantation

f

Tumor volume (mm^3)

N.S. ($P = 0.901$)

DGFP   mMeflin/DGFP

SeV

g

IHC: CD31

SeV: DGFP   SeV: mMeflin/DGFP

100 μm

h

Blood vessel lumen area (μm^2) /200× field

$P < 0.0001$

DGFP (4 mice)   mMeflin/DGFP (4 mice)

CD31$^+$ area ($\times 10^3$ μm^2) /200× field

$P < 0.0001$

DGFP (4 mice)   mMeflin/DGFP (4 mice)

i

Tumor volume (50–100 mm^3) (Day 0)

Gem (50 mg/Kg)

C57BL/6J (N = 7/each group)

1   5   8 9 11   14   17 (Day)

SeV (DGFP or mMeflin/DGFP)
Intratumoral injection

mT5 subcutaneous transplantation

j

Tumor volume (mm^3)

$P = 0.0148$

DGFP   mMeflin/DGFP

SeV

(Fig. 4a). The combined treatment did not affect the body weight of mice (Fig. 4b). Interestingly, Am80 administration enhanced the antitumor effects of Gem, as demonstrated by monitoring of tumor volume and weight (Fig. 4c, d). Histological analysis using hematoxylin and eosin staining showed that tumors treated with the combination therapy contained a greater number of necrotic cells with pyknotic nuclei (Fig. 4e) and exhibited higher Meflin and lower α-SMA expression than tumors treated with Gem alone (Fig. 4f–g). Consistent with the effects of Am80 administration on tumor vessel area (Fig. 3g), the concentration of Gem (2′,2-difluorodeoxycytidine [dFdC]) was higher in tumors treated with the combination therapy than in those treated with Gem

Fig. 2 SeV-mediated transduction of Meflin induced increases in tumor vessel area and sensitivity to Gem. a, b Recombinant SeV encoding DasherGFP (DGFP) or mouse Meflin and DGFP (mMeflin/DGFP) was used to infect mouse MSCs, followed by western blot (WB) analysis with the indicated antibodies (**a**) and quantitative PCR (qPCR) for the indicated genes (**b**). *Mr*, molecular marker. **c** WT female mice (P42) were subcutaneously transplanted with mT5 mouse PDAC cells (1×10^6 cells/mouse), followed by intratumoral injection of the indicated SeV (3×10^7 CIU) at day 12 and sacrifice at day 19. **d** Observation of GFP fluorescence in frozen sections prepared from mT5 tumors infected with SeV encoding DGFP (left) and Meflin/DGFP (right) (upper panel). FFPE sections were also obtained from tumors and stained for Meflin (*Islr*) and α-SMA (*Acta2*) by ISH (middle and lower panels). Arrows indicate Meflin+ or *Acta2*+ CAFs. **e–h** mT5 tumors transplanted into WT female mice (P42) were allowed to grow until reaching 50–100 mm³ in volume. Mice were then injected with SeV encoding DGFP or Meflin/DGFP three times every 4 days and sacrificed on day 17 (**e**). Tumor volume was measured (**f**), and IHC for CD31 was performed to quantify the tumor vessel lumen and CD31+ area (**g, h**). **i, j** mT5 tumors transplanted into WT female mice (P42) were allowed to grow until reaching 50–100 mm³ in volume (day 0). Mice were then injected with SeV encoding DGFP or Meflin/DGFP three times every 4 days (days 1, 5, and 9). The mice were i.p. administered Gem four times on days 5, 8, 11, and 14 and then sacrificed on day 17 (**i**). Tumor volume was measured (**j**).

---

monotherapy, suggesting that Am80 enhanced the intratumoral delivery of Gem (Fig. 4h). In contrast to mT5 tumors infected with SeV-Meflin, the effects of Am80 administration on collagen deposition in the tumor stroma were eliminated by Gem treatment (Supplementary Fig. 9b).

The effects of oral Am80 administration were further tested using an orthotopic PDAC model, in which we transplanted mT5 cells into the pancreas of WT mice (Fig. 5a). Measurement of the tumor sizes and weights of the developed tumors revealed that Am80 administration significantly improved the antitumor effects of Gem, accompanied by an increase in the number of necrotic tumor cells (Fig. 5b–e). Am80 administration increased blood vessel areas in the developed tumors without affecting those in the normal pancreas (Supplementary Fig. 10a, b). Meflin expression was increased, whereas α-SMA expression and collagen deposition were downregulated by Am80 administration irrespective of Gem treatment, further supporting the notion that Am80 administration may promote the formation of a tumor-restraining TME that improves tumor sensitivity to chemotherapeutics (Fig. 5f–h, Supplementary Fig. 10c).

The benefit of oral Am80 administration was also confirmed using the KPC PDAC mouse model, which recapitulates human PDAC with extensive stromal fibroinflammatory reaction [28] (Supplementary Fig. 11). KPC mice administered the Am80 and Gem combination exhibited better survival than those administered either control or Gem alone.

We next transplanted BxPC3 human PDAC cells into immunocompromised nude mice, followed by oral administration of Am80 and the combination chemotherapy of Gem and nabPTX (Supplementary Figs. 12, 13). Am80 administration did not alter the body weight of mice but significantly improved the antitumor effects of Gem plus nabPTX, accompanied by an increase in Meflin expression and a decrease in α-SMA expression (Supplementary Figs. 12a–d, 13a, b). This observation suggested minor involvement of the immune machinery in the mechanism of action. Consistent with the subcutaneous mT5 model, increased collagen deposition induced by Gem plus nabPTX combination therapy was not reversed by Am80 administration (Supplementary Fig. 13c).

Am80-mediated enhancement of chemosensitivity required Meflin expression in CAFs

Next, to further confirm the significance of Am80-mediated Meflin expression in enhanced chemosensitivity, we transplanted mT5 cells into Meflin-KO mice, followed by Am80 administration and Gem treatment (Fig. 6a). Gem treatment, with or without Am80 administration, did not alter the body weight of the transplanted Meflin-KO mice (Fig. 6b). Am80 administration in combination with Gem resulted in no statistically significant decrease in tumor volume and weight compared with Gem monotherapy (Fig. 6c, d). The numbers of necrotic cells with pyknotic nuclei and the expression levels of α-SMA in the stroma were comparable between the monotherapy and combination therapy groups (Fig. 6e–h). Because Meflin is specifically expressed in CAFs but not

other cell types in PDAC tissue [20], these data suggested that Am80 exerted its effects on chemotherapeutic efficacy by upregulation of Meflin in CAFs.

Meflin interacted with lysyl oxidase (Lox) to suppress its collagen crosslinking activity

Meflin augments bone morphogenetic protein (BMP) 7 signaling to oppose the profibrotic action of transforming growth factor-β [37, 38]; however, this mechanism does not fully explain the changes found in tumors administered Am80 and the differences between WT and Meflin-KO tumors. In our previous reports, second-harmonic generation (SHG) microscopic observations revealed that the stroma of tumors in Meflin-KO KPC mice exhibited significant remodeling of collagen architectures compared with those in WT KPC mice [20]. These data suggested that Meflin was involved in regulation of the collagen configuration in the tumor stroma, which may subsequently change the mechanical properties of the tumor stroma, such as interstitial pressure [39].

To identify the mechanisms through which Meflin is involved in regulation of stromal collagen, we attempted to identify novel ligands of Meflin. To this end, we transduced mouse MSCs with Meflin cDNA tagged with the hemagglutinin (HA) epitope, followed by immunoprecipitation (IP) with anti-HA antibodies and analysis of the eluate by mass spectrometry (Supplementary Fig. 14a, b). We identified seven secreted or membrane proteins as candidate Meflin interactors and focused on the protein with the highest score, Lox (Supplementary Fig. 14c). Lox is known to crosslink collagen and elastin, the two major components of the ECM, contributing to the stiffness and interstitial pressure of the tumor stroma [40, 41]. IP assays confirmed that Meflin interacted with Lox (Fig. 7a) and Lox like 2 (Loxl2), another member of the *Lox* gene family (Supplementary Fig. 14d). Direct interaction of Meflin and Lox was demonstrated in in vitro binding assays using purified recombinant Meflin and Lox proteins (Supplementary Fig. 14e). Additional IP assays revealed the interaction of endogenous Meflin with Lox and Loxl2 proteins, highlighting the physiological relevance of these protein interactions (Fig. 7b, Supplementary Fig. 14f). A mutant Lox lacking the amino-terminal pro-sequence also interacted with Meflin, suggesting that the catalytic domain (CD) of Lox was responsible for this interaction (Fig. 7c, d). Pull-down assays using Meflin mutants fused with the constant region (Fc) of human immunoglobulin lacking one of the leucine-rich repeats (LRRs) and the immunoglobulin (Ig)-like domain showed that a region spanning the LRR1–4 domains of Meflin was likely to be responsible for Lox binding (Supplementary Fig. 15a, b). Functionally, biochemical assays showed that Meflin had inhibitory effects on the oxidative deamination activity of Loxl2, suggesting that Meflin had inhibitory roles in collagen crosslinking mediated by Lox or Loxl2 (Fig. 7e).

We next analyzed the effects of Am80 administration on the collagen signature of mT5 xenograft tumors in the presence or absence of Gem by SHG microscopy (Fig. 7f, g). The data showed highly aligned collagen fibers in control mT5 tumors, which were significantly reversed by Am80 administration, in the absence of
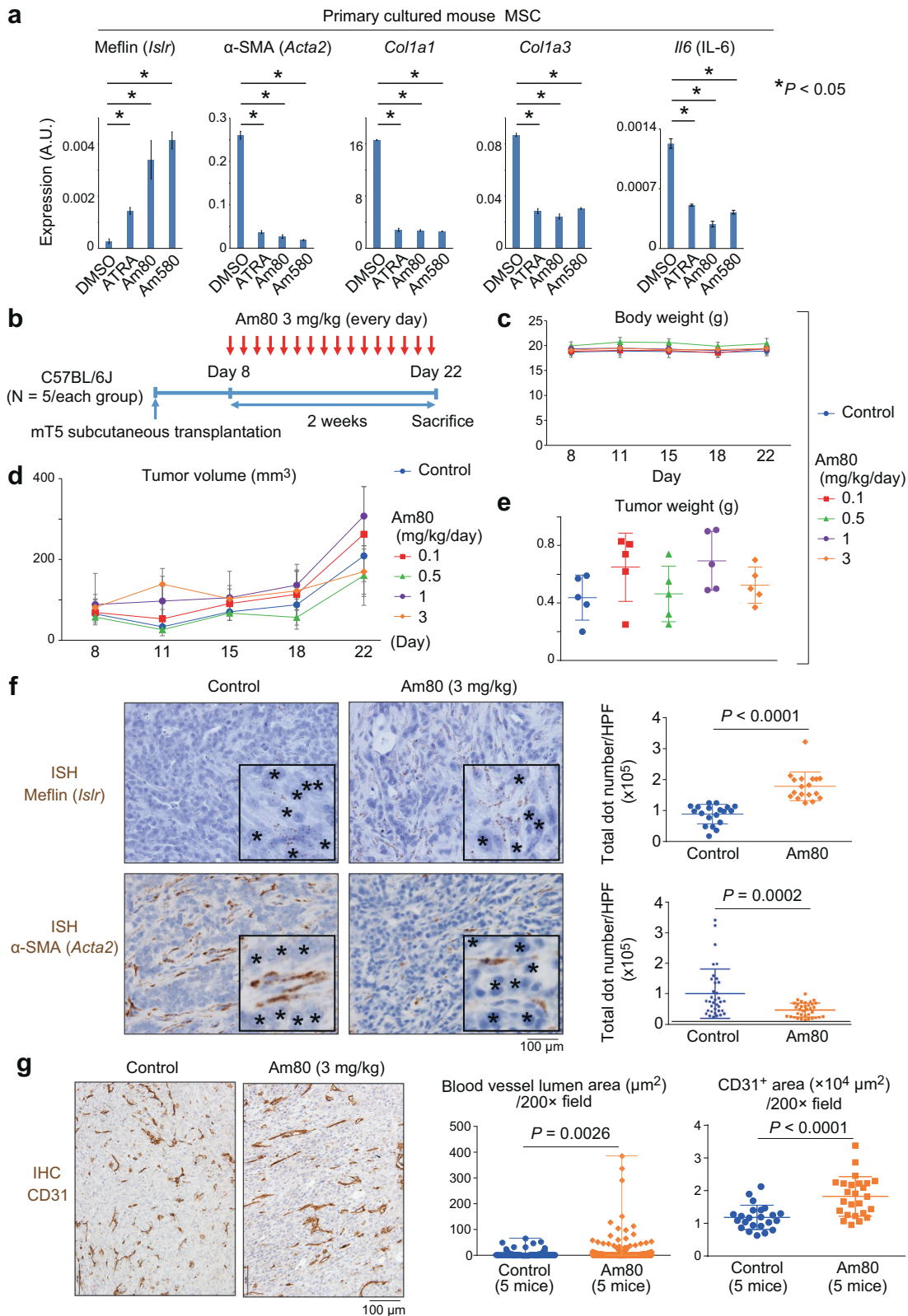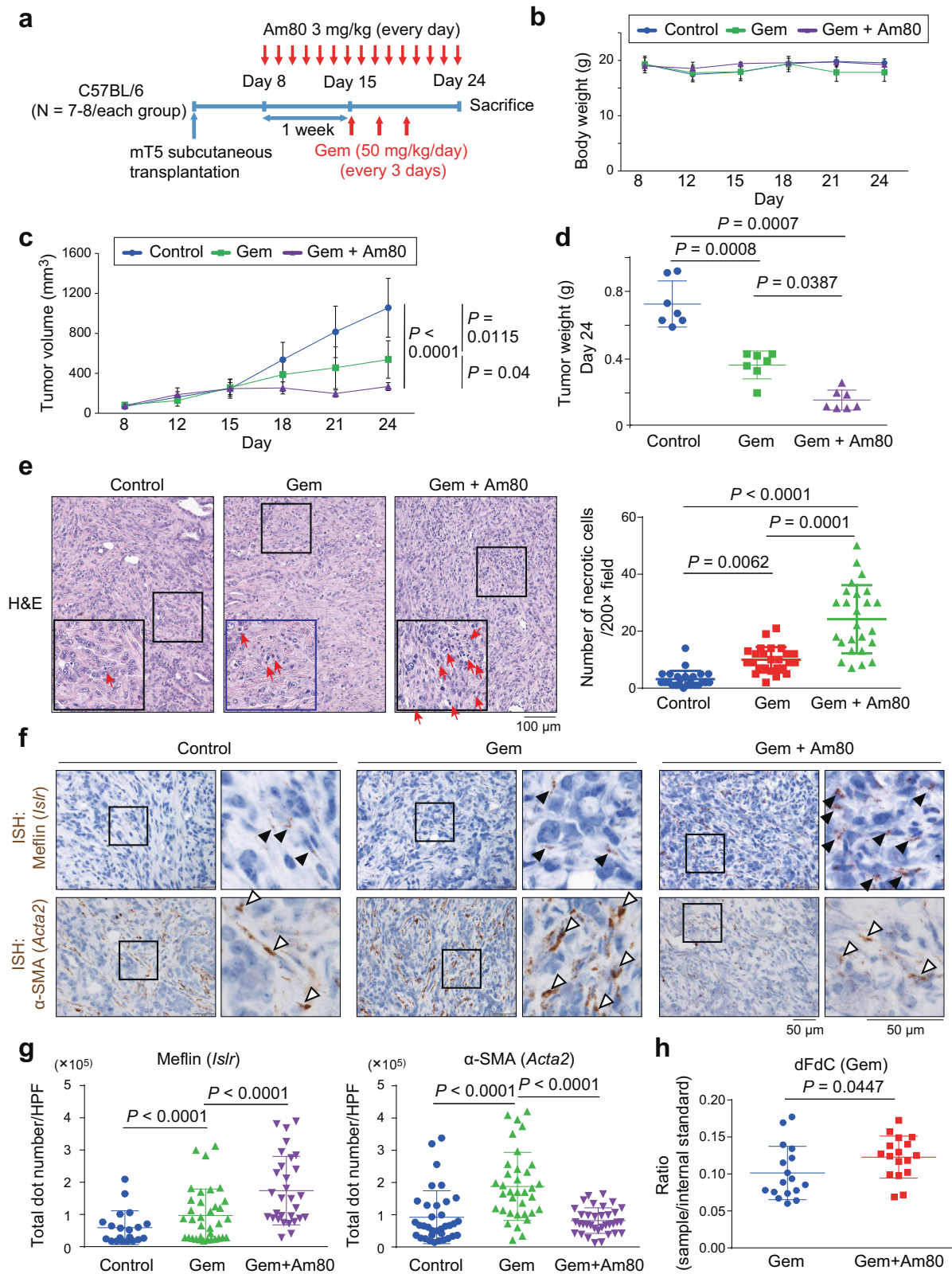
Fig. 3 Effects of Am80 administration on the expression of Meflin in CAFs and on tumor vessel area in a PDAC xenograft mouse model. **a** Primary cultured mouse MSCs were plated in the presence of DMSO, ATRA, Am80, and AM580 for 48 h, and qPCR of the indicated genes was performed. **b–e** WT female mice (P42) were subcutaneously transplanted with mT5 mouse PDAC cells (1×10^6 cells/mouse), followed by oral administration of Am80 (3 mg/kg, 0.5% carboxymethylcellulose [CMC] solution) every day for 14 days (**b**). Body weights of mice (**c**) and tumor volumes (**d**) were measured during the observation period. **e** Tumor weight on the day of sacrifice (day 22). **f, g** Tissue sections prepared from control mT5 tumors (left) and those administered Am80 (right) were examined for Meflin and α-SMA expression by ISH (**f**) and for CD31 expression by IHC (**g**). Meflin and α-SMA expression levels (**f**) and tumor vessel lumen and CD31$^+$ areas (**g**) were calculated. For quantification of ISH signals, the number of dots per high-power (400×) microscopic field (HPF) was counted, and 20 HPFs randomly selected from five animals were evaluated for each group. Asterisks denote tumor cells that were negative for Meflin and α-SMA expression.

a C57BL/6 (N = 7-8/each group); mT5 subcutaneous transplantation; Am80 3 mg/kg (every day), Day 8, Day 15, Day 24, Sacrifice; 1 week; Gem (50 mg/kg/day) (every 3 days)

b Body weight (g) vs Day; Control, Gem, Gem + Am80

c Tumor volume (mm³) vs Day; Control, Gem, Gem + Am80; P < 0.0001; P = 0.0115; P = 0.04

d Tumor weight (g) Day 24; P = 0.0007; P = 0.0008; P = 0.0387; Control, Gem, Gem + Am80

e H&E; Control, Gem, Gem + Am80; 100 µm; Number of necrotic cells /200× field; P < 0.0001; P = 0.0001; P = 0.0062; Control, Gem, Gem + Am80

f ISH: Meflin (*Islr*); ISH: α-SMA (*Acta2*); Control, Gem, Gem + Am80; 50 µm, 50 µm

g Meflin (*Islr*) (×10⁵); Total dot number/HPF; P < 0.0001; P < 0.0001; Control, Gem, Gem+Am80. α-SMA (*Acta2*) (×10⁵); Total dot number/HPF; P < 0.0001; P < 0.0001; Control, Gem, Gem+Am80

h dFdC (Gem); Ratio (sample/internal standard); P = 0.0447; Gem, Gem+Am80

Gem treatment. This difference disappeared upon Gem treatment. Other collagen signatures, such as curvature, width, and fiber length, were all comparable between the tested groups (Supplementary Fig. 16a–c). The effects of Am80 on collagen fiber alignment in the absence of Gem treatment were also observed in the orthotopic PDAC model, although statistical significance was not reached (Supplementary Fig. 17a, b). Interestingly, measurement of the Young's modulus of the tumors showed that Am80-treated tumors were softer than control tumors (Fig. 7h, i). Because collagen fiber alignment modulates tumor stiffness [39], these

Fig. 4 Am80 administration improved tumor sensitivity to Gem and induced Meflin expression in CAFs in a subcutaneous PDAC xenograft mouse model. a WT female mice (P42) were subcutaneously transplanted with mT5 mouse PDAC cells (1×10^6 cells/mouse) on day 0, followed by oral administration of Am80 from day 8 for 16 consecutive days. The mice were administered Gem from day 15 three times every 3 days and sacrificed on day 24. **b–d** Measurement of the body weights of mice (**b**) and tumor volumes (**c**) during the observed period and of tumor weights on day 24 (**d**). **e** Representative images of H&E-stained tissue sections of tumors prepared from the indicated groups. Boxed regions are magnified in insets. Arrows denote necrotic cells with pyknotic nuclei. The numbers of necrotic cells were counted and quantified in the graph shown in the right panel. Twenty-five images obtained from five tumors per group using a 20× objective lens were analyzed and quantified. **f, g** Tissue sections of tumors from the indicated groups were stained for Meflin and α-SMA by ISH (**f**), followed by quantification of total dot numbers (**g**). Open and solid arrowheads denote Meflin$^+$ and α-SMA$^+$ CAFs, respectively. **h** Quantification of dFdC (Gem) delivered to tumors in the indicated groups after administration of Gem three times. Lysates prepared from mT5 tumors treated with Gem ($n = 17$) and Gem plus Am80 ($n = 17$) were added to stable isotope-labeled dFdC (internal control) and subjected to liquid chromatography-mass spectrometry analysis, followed by quantification of dFdC and the internal control. The data are expressed as relative ratios of dFdC to the internal control.

data suggested that Am80-mediated Meflin upregulation inhibited Lox-mediated collagen crosslinking, thereby controlling the physical properties of tumors (Fig. 7j).

Differential effects of Am80 and vitamin D administration on CAF gene expression

Administration of the vitamin D analogue calcipotriol alters the gene expression of stromal cells of PDAC in mice [31]. Therefore, we next investigated how Am80 differed from vitamin D analogues in terms of effects on gene expression in PDAC CAFs. Thus, we stimulated primary cultured PSCs isolated from three patients with PDAC (PSC163, PSC52, and PSC119) with dimethyl sulfoxide (DMSO, control), Am80, or calcipotriol. Gene expression profiles were then compared using microarray-based transcriptomic analysis (acc. no. GSE179318; Supplementary Fig. 18a, b). Extracting genes that were differentially expressed between Am80- and calcipotriol-treated cells revealed that Meflin expression was more significantly upregulated by Am80 than calcipotriol. Interestingly, the expression levels of fibroblast activation protein and chemokine (C-C motif) ligand 2, which are markers of pCAFs [2, 6, 7, 42, 43], were higher in Am80-treated PSCs than in calcipotriol-treated PSCs, whereas the expression levels of other pCAF marker genes, such as C-X-C motif chemokine ligand 12, podoplanin, and periostin, were higher in calcipotriol-treated cells. These data suggested that Am80 and calcipotriol differentially regulated gene expression in PSCs.

DISCUSSION

In the current study, we found that the number of Meflin$^+$ CAFs, a candidate for rCAFs in PDAC, correlated with the response of patients with PDAC to chemotherapies. We also demonstrated the tumor-suppressive role of Meflin in PDAC mouse models by inducing its expression through genetic and pharmacological approaches. These experiments led to the identification of Am80 as an inducer of Meflin expression in CAFs and showed that Am80 improved the sensitivity of PDAC to chemotherapeutics. Finally, we showed that Meflin functioned to suppress Lox collagen crosslinking activity, which may increase tumor vessel area and chemotherapeutic sensitivity, as observed in tumors with high Meflin expression (Fig. 7j). Taken together, these data support that there are functionally heterogeneous but phenotypically plastic subsets of CAFs in the tumor stroma, consistent with the observation that tumor immunity is regulated by the net balance of anti- and protumor immune cells [44, 45]. Given that Meflin$^+$ CAFs weakly or moderately express α-SMA [7, 20], we speculate that the failure to deplete all α-SMA$^+$ CAFs in a preclinical PDAC model was caused by the depletion of Meflin$^+$ CAFs [10]. One of the limitations of the current study is that it mainly relied on the results of subcutaneous and orthotopic transplantation assays, and further experiments on the KPC autochthonous PDAC model and larger clinical samples will be needed to validate our conclusions.

The findings in the current study should be discussed in the context of a previous study in which researchers demonstrated that calcipotriol administration suppresses stromal activation and improves the efficacy of Gem treatment in a PDAC mouse model [31]. Calcipotriol targets activated PSCs expressing vitamin D receptor (VDR), which likely represent pCAFs, to revert or deactivate them to a more quiescent, less cancer-supportive state [20, 31]. This VDR- and ligand-mediated reversion of activated PSCs to quiescent PSCs has been called stromal reprogramming, which is the basis of ongoing clinical trials that test the efficacy of vitamin D analogues in combination with chemotherapeutics or immune checkpoint inhibitors in patients with PDAC (www.clinicaltrials.gov). We previously reported that Meflin is a marker of quiescent PSCs in the normal pancreas, and its expression was upregulated by calcipotriol [20]. This was consistent with the results of the current study showing that Meflin expression in CAFs was correlated with sensitivity to chemotherapeutics in PDAC. Therefore, Meflin may be a surrogate or monitoring marker of the stromal reprogramming of PDAC in clinical trials.

Am80 is a synthetic unnatural retinoid that specifically binds to RARα and β, with Ki values of 6.5×10^{-9} and 3.0×10^{-10} M, respectively, but not RARγ; these findings are contradictory to those for ATRA, which has similar affinities to all RAR isoforms [46]. In addition, Am80 shows several pharmacological advantages over ATRA. For example, Am80 exhibits significantly higher stability to light, heat, and oxidation than ATRA, enabling a lower dose (6 mg/m^2) to be used to achieve efficacy compared with ATRA (45 mg/m^2) in clinical practice [36]. Am80 binds to cellular RA-binding protein, the induced upregulation of which is known to mediate resistance to ATRA in APL, with a 20-fold lower affinity than ATRA [36, 46]. Oral intake of Am80 does not produce serious metabolic complications, such as hypercalcemia caused by high-dose vitamin D administration [47]. Furthermore, similar to ATRA, Am80 has been shown to have various biological activities, including induction of cell differentiation and modulation of immunity [33, 48]. Therefore, the hypothesis that Am80 suppresses tumor progression by increasing the number of Meflin$^+$ rCAFs may be a simplistic interpretation of the experimental results obtained in the current study, and more extensive studies are needed to comprehensively elucidate the effects of Am80 on tumor cells and TME components. Additionally, it will be necessary to evaluate the effects of Am80 oral administration on drug sensitivity in patients with PDAC in the clinical setting.

Our data showed a significant increase in blood vessel areas in tumors treated with SeV-Meflin and Am80, supporting the involvement of these interventions in modulation of tumor angiogenesis. However, previous studies showed an inhibitory effect of Am80 on angiogenesis [49] and no Meflin expression in vascular endothelial and smooth muscle cells [21]; thus, it is plausible that SeV-Meflin- and Am80-mediated changes in the tumor vessel lumen may be attributed to alterations in the mechanical properties of the tumor stroma. Consistent with this hypothesis, our search for Meflin ligands revealed that Meflin
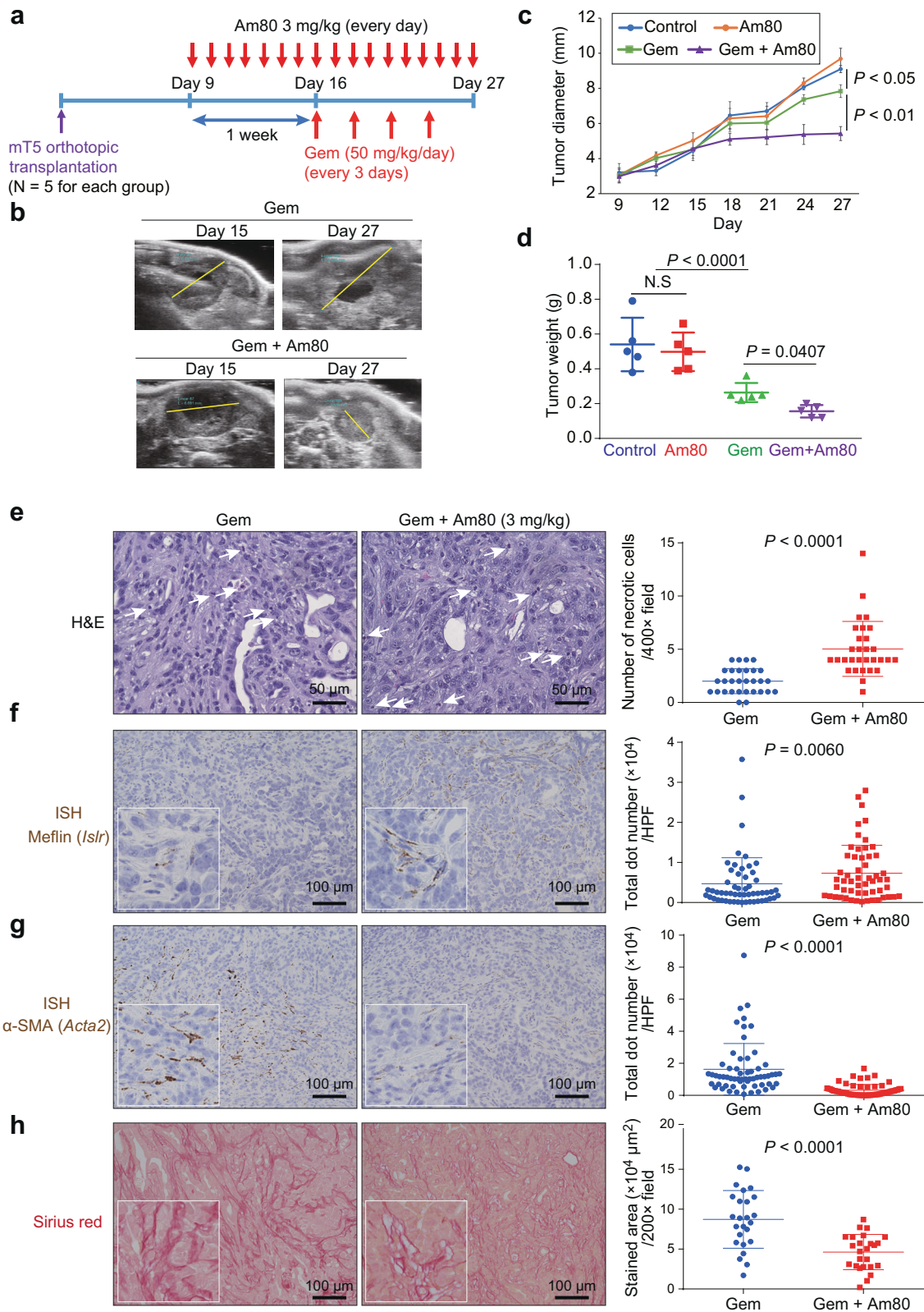
Fig. 5   Am80 administration improved tumor sensitivity to Gem and induced Meflin expression in CAFs in an orthotopic PDAC xenograft mouse model. a mT5 mouse PDAC cells (1×10^3 cells/mouse) were orthotopically transplanted into the pancreas of WT female mice (P42), followed by oral administration of Am80 from day 9 for 27 consecutive days. The mice were administered Gem from day 16 three times every 3 days and sacrificed on day 27. **b–d** Measurement of tumor diameters by ultrasound imaging during the observed period (**b**, **d**) and tumor weights on day 19 (**d**). **e** Representative images of H&E-stained tissue sections of tumors prepared from the indicated groups. Arrows denote necrotic cells with pyknotic nuclei. The numbers of necrotic cells were counted and quantified in the graph shown in the right panel. Thirty images obtained from five tumors per group using a 40× objective lens were analyzed and quantified. **f, g, h** Tissue sections of tumors from the indicated groups were stained for Meflin and α-SMA by ISH (**f, g**) and collagen fibers by Sirius-red staining (**h**), followed by quantification.
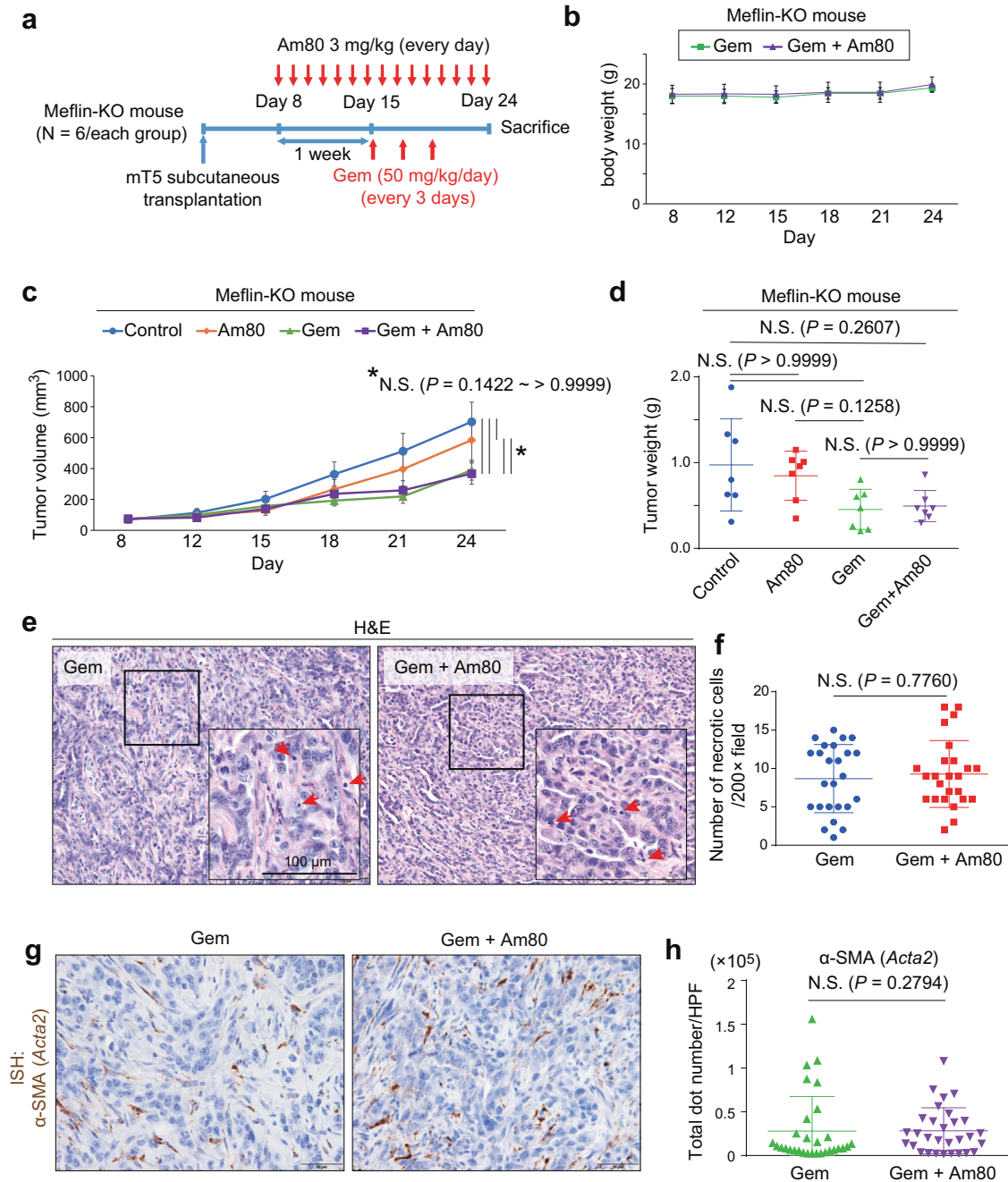
Fig. 6 Increased tumor chemosensitivity by Am80 administration was mediated by alterations in Meflin expression in CAFs. a Meflin-KO female mice (P42) were subcutaneously transplanted with mT5 mouse PDAC cells (1 × 10⁶ cells/mouse) on day 0, followed by oral administration of Am80 from day 8 for 16 consecutive days. Mice were administered Gem from day 15 three times every 3 days and sacrificed on day 24. **b–d** Measurement of the body weights of mice (**b**) and tumor volumes (**c**) during the observation period, and tumor weights on day 24 (**d**). **e, f** Representative images of H&E-stained tissue sections of tumors prepared from the indicated groups (**e**). Boxed regions are magnified in insets. Arrows denote necrotic cells with pyknotic nuclei. The numbers of necrotic cells were counted and quantified in the graph shown in (**f**). **g, h** Tissue sections of tumors from the indicated groups were stained for α-SMA by ISH (**g**), followed by quantification of total dot numbers (**h**).

interacts with Lox to inhibit its collagen crosslinking activity. Lox is a critical regulator of the physical properties of the tumor stroma, such as stiffness and interstitial pressure [39]. Therefore, artificial induction of Meflin expression in CAFs may be a rational approach to improve the perfusion of tumor vessels and drug delivery. The involvement of other reported functions of Meflin, including the regulation of BMP7, Wnt, and Hippo-Yes-associated protein

signaling pathways, in the regulation of tumor vessel area also needs to be considered [50, 51].

In conclusion, our current findings showed that Meflin expression in CAFs improved tumor sensitivity to chemotherapeutics, consistent with our previous studies identifying Meflin as a marker of rCAFs, which are functionally different from protumorigenic pCAFs. Consistent with this, the induction of
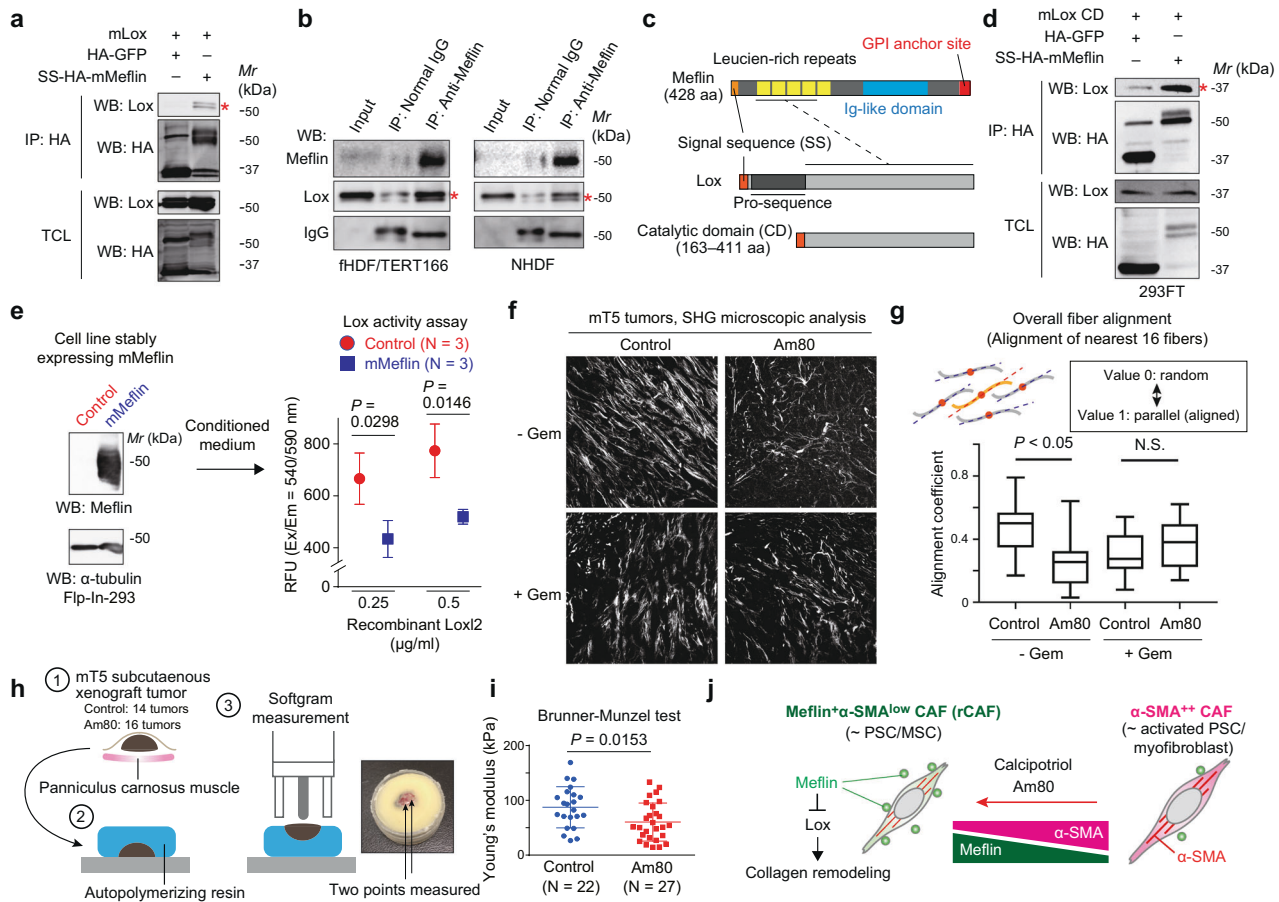
Fig. 7 Meflin was involved in the regulation of Lox activity and collagen remodeling. a The indicated plasmids were transfected into HEK293 cells, and cell lysates were then subjected to IP with anti-HA antibodis and western blot analysis. Lox coprecipitated with HA-Meflin (asterisk). mMeflin mouse Meflin, mLox mouse Lox, SS signal sequence, TCL total cell lysate. **b** Interaction of endogenous Meflin and Lox proteins. Cell lysates prepared from the fHDF/TERT166 fibroblast cell line (left) or primary cultured human fibroblasts (NHDFs, right) were immunoprecipitated with anti-Meflin antibodies, followed by analysis of eluates by WB with the indicated antibodies. Lox proteins coprecipitated with Meflin (asterisk). **c** Primary structure of human Meflin (top) and mouse Lox (middle). Lox comprises an amino-terminal SS, a pro-sequence, and a catalytic domain (CD). (Bottom) Construct encoding the CD of Lox with an SS at the amino terminus. Dashed line: protein domains responsible for the Lox/Meflin interaction. **d** The indicated plasmids were cotransfected into 293FT cells, followed by IP with anti-HA antibodies and WB analysis. Meflin interacted with the CD of mLox (asterisk). **e** Conditioned medium from control Flp-In-293 cells or Flp-In-293 cells stably expressing mMeflin was mixed with recombinant Loxl2 (0.25 and 0.5 μg/mL), followed by measurement of hydrogen peroxide using a fluorometric-based method. (Left) WB analysis of Meflin expression in Flp-In-293 cells. RFU, relative fluorescence unit. **f**, **g** Measurement of collagen alignment in the stroma of subcutaneous mT5 tumors developed in mice by SHG microscopy. Eight to sixteen images from tissue sections of control tumors and tumors treated with Am80 were analyzed. Representative images (**f**) and quantification of collagen alignment (**g**). **h**, **i** Measurement of the stiffness of mT5 tumors developed in control mice ($n = 14$) and those treated with Am80 ($n = 16$). The Young's modulus of the flat surfaces of tumors contacting the fascia of the panniculus carnosus muscle were measured (**h**). One or two points were selected in each tumor, and each point was measured more than 5 times; quantification was performed (**i**). **j** Schematic diagram showing the working hypothesis for the mechanism of Am80-mediated alteration in tumor sensitivity to chemotherapeutics.

Meflin expression by either genetic or pharmacological approaches improved tumor sensitivity to chemotherapeutics in a PDAC xenograft model. Taken together, these data provide a rationale for therapeutic strategies that increase the number of rCAFs in the treatment of patients with PDAC.

MATERIALS AND METHODS
Human tissue samples
All human PDAC samples were obtained at the time of endoscopic ultrasound-guided fine needle aspiration after the patients had provided informed consent. This study was approved by the Ethics Committee of Nagoya University Graduate School of Medicine (approval number 2017-0127-3).

Animals
All animal protocols were reviewed and approved by the Animal Care and Use Committee of Nagoya University Graduate School of Medicine (approval numbers 30366 and 20409), and studies were conducted in compliance with institutional and national guidelines. The establishment of KPC model and Meflin-knockout (KO) mice was described previously [20, 21]. Genomic DNA extracted from mouse tails was used for polymerase chain reaction (PCR)-based genotyping of wild-type (WT) and Meflin-KO mice. The sequences of the primers used for genotyping of the Meflin (Islr) gene were as follows: PCR1 forward, 5′-GCTGCATTTGAGCTGAGCCTCTGG-3′; PCR1 reverse, 5′-AACCCCTTCCTCCTACATAGTTGG-3′; PCR2 forward, 5′-TGAGGTTAGCCTGGGGACTTCAC-3′; PCR2 reverse, 5′-GGCTAGAACTCT CAAAGTAGGTCAGG-3′.

Recombinant virus generation, animal experiments, histology, cell biology, biochemistry, mass spectrometric analysis, and statistical analysis
Detailed protocols for recombinant virus generation, animal experiments, histology, cell biology, biochemistry, mass spectrometric analysis, and statistical analysis are described in the Supplementary Data.

REFERENCES

1. Apte MV, Park S, Phillips PA, Santucci N, Goldstein D, Kumar RK, et al. Desmoplastic reaction in pancreatic cancer: role of pancreatic stellate cells. Pancreas. 2004;29:179–87.
2. Sahai E, Astsaturov I, Cukierman E, DeNardo DG, Egeblad M, Evans RM, et al. A framework for advancing our understanding of cancer-associated fibroblasts. Nat Rev Cancer. 2020;20:174–86.
3. Neesse A, Bauer CA, Öhlund D, Lauth M, Buchholz M, Michl P, et al. Stromal biology and therapy in pancreatic cancer: ready for clinical translation? Gut 2019;68:159–71.
4. Öhlund D, Elyada E, Tuveson D. Fibroblast heterogeneity in the cancer wound. J Exp Med. 2014;211:1503–23.
5. Gieniec KA, Butler LM, Worthley DL, Woods SL. Cancer-associated fibroblasts—heroes or villains? Br J Cancer. 2019;121:293–302.
6. Kobayashi H, Enomoto A, Woods SL, Burt AD, Takahashi M, Worthley DL. Cancer-associated fibroblasts in gastrointestinal cancer. Nat Rev Gastroenterol Hepatol. 2019;16:282–95.
7. Miyai Y, Esaki N, Takahashi M, Enomoto A. Cancer-associated fibroblasts that restrain cancer progression: hypotheses and perspectives. Cancer Sci. 2020;111:1047–57.
8. Ishii G, Ochiai A, Neri S. Phenotypic and functional heterogeneity of cancer-associated fibroblast within the tumor microenvironment. Adv Drug Deliv Rev. 2016;99:186–96.
9. Mezawa Y, Orimo A. The roles of tumor-and metastasis-promoting carcinoma-associated fibroblasts in human carcinomas. Cell Tissue Res. 2016;365:675–89.
10. Özdemir BC, Pentcheva-Hoang T, Carstens JL, Zheng X, Wu CC, Simpson TR, et al. Depletion of carcinoma-associated fibroblasts and fibrosis induces immunosuppression and accelerates pancreas cancer with reduced survival. Cancer Cell. 2014;25:719–34.
11. Rhim AD, Oberstein PE, Thomas DH, Mirek ET, Palermo CF, Sastra SA, et al. Stromal elements act to restrain, rather than support, pancreatic ductal adenocarcinoma. Cancer Cell. 2014;25:735–47.
12. Lee JJ, Perera RM, Wang H, Wu DC, Liu XS, Han S, et al. Stromal response to Hedgehog signaling restrains pancreatic cancer progression. Proc Natl Acad Sci USA. 2014;111:E3091–100.
13. Bhattacharjee S, Hamberger F, Ravichandra A, Miller M, Nair A, Affo S, et al. Tumor restriction by type I collagen opposes tumor-promoting effects of cancer-associated fibroblasts. J Clin Investig. 2021;131:e146987.
14. Chen Y, Kim J, Yang S, Wang H, Wu CJ, Sugimoto H, et al. Type I collagen deletion in αSMA+ myofibroblasts augments immune suppression and accelerates progression of pancreatic cancer. Cancer Cell. 2021;39:548–65.
15. Biffi G, Oni TE, Spielman B, Hao Y, Elyada E, Park Y, et al. IL1-induced JAK/STAT signaling is antagonized by TGFβ to shape CAF heterogeneity in pancreatic ductal adenocarcinoma. Cancer Discov. 2019;9:282–301.
16. Elyada E, Bolisetty M, Laise P, Flynn WF, Courtois ET, Burkhart RA, et al. Cross-species single-cell analysis of pancreatic ductal adenocarcinoma reveals antigen-presenting cancer-associated fibroblasts. Cancer Discov. 2019;9:1102–23.
17. Öhlund D, Handly-Santana A, Biffi G, Elyada E, Almeida AS, Ponz-Sarvise M, et al. Distinct populations of inflammatory fibroblasts and myofibroblasts in pancreatic cancer. J Exp Med. 2017;214:579–96.
18. Shi Y, Gao W, Lytle NK, Huang P, Yuan X, Dann A, et al. Targeting LIF-mediated paracrine interaction for pancreatic cancer therapy and monitoring. Nature. 2019;569:131–5.
19. Nagathihalli NS, Castellanos JA, VanSaun MN, Dai X, Ambrose M, Guo Q, et al. Pancreatic stellate cell secreted IL-6 stimulates STAT3 dependent invasiveness of pancreatic intraepithelial neoplasia and cancer cells. Oncotarget. 2016;7:65982–92.
20. Mizutani Y, Kobayashi H, Iida T, Asai N, Masamune A, Akitoshi H, et al. Meflin-positive cancer-associated fibroblasts inhibit pancreatic carcinogenesis. Cancer Res. 2019;79:5367–81.
21. Maeda K, Enomoto A, Hara A, Asai N, Kobayashi T, Horinouchi A, et al. Identification of Meflin as a potential marker for mesenchymal stromal cells. Sci Rep. 2016;6:22288.
22. Takahashi M, Kobayashi H, Mizutani Y, Hara A, Iida T, Miya Y, et al. Roles of the mesenchymal stromal/stem cell marker Meflin/Islr in cancer fibrosis. Front Cell Dev Biol. 2021;9:749924.
23. Hara A, Kato K, Ishihara T, Kobayashi H, Asai N, Mii S, et al. Meflin defines mesenchymal stem cells and/or their early progenitors with multilineage differentiation capacity. Genes Cells. 2021;26:495–512.
24. Neuzillet C, Tijeras-Raballand A, Ragulan C, Cros J, Patil Y, Martinet M, et al. Inter- and intra-tumoural heterogeneity in cancer-associated fibroblasts of human pancreatic ductal adenocarcinoma. J Pathol. 2019;248:51–65.
25. Waghray M, Yalamanchili M, Dziubinski M, Zeinali M, Erkkinen M, Yang H, et al. GM-CSF mediates mesenchymal–epithelial cross-talk in pancreatic cancer. Cancer Discov. 2016;6:886–99.
26. Quante M, Tu SP, Tomita H, Gonda T, Wang SSW, Takashi S, et al. Bone marrow-derived myofibroblasts contribute to the mesenchymal stem cell niche and promote tumor growth. Cancer Cell. 2011;19:257–72.
27. Boj SF, Hwang CI, Baker LA, Chio II, Engle DD, Corbo V, et al. Organoid models of human and mouse ductal pancreatic cancer. Cell. 2015;160:324–38.
28. Hingorani SR, Wang L, Multani AS, Combs C, Deramaudt TB, Hruban RH, et al. Trp53R172H and KrasG12D cooperate to promote chromosomal instability and widely metastatic pancreatic ductal adenocarcinoma in mice. Cancer Cell. 2005;7:469–83.
29. Zhang D, Li L, Jiang H, Li Q, Wang-Gillam A, Yu J, et al. Tumor-stroma IL1β-IRAK4 feedforward circuitry drives tumor fibrosis, chemoresistance, and poor prognosis in pancreatic cancer. Cancer Res. 2018;78:1700–12.
30. Olive KP, Jacobetz MA, Davidson CJ, Gopinathan A, McIntyre D, Honess D, et al. Inhibition of Hedgehog signaling enhances delivery of chemotherapy in a mouse model of pancreatic cancer. Science. 2009;324:1457–61.
31. Sherman MH, Yu RT, Engle DD, Ding N, Atkins AR, Tiriac H, et al. Vitamin D receptor-mediated stromal reprogramming suppresses pancreatitis and enhances pancreatic cancer therapy. Cell. 2014;159:80–93.
32. Chronopoulos A, Robinson B, Sarper M, Cortes E, Auernheimer V, Lachowski D, et al. ATRA mechanically reprograms pancreatic stellate cells to suppress matrix remodelling and inhibit cancer cell invasion. Nat Commun. 2016;7:12630.
33. Kocher HM, Basu B, Froeling FEM, Sarker D, Slater S, Carlin D, et al. Phase I clinical trial repurposing all-trans retinoic acid as a stromal targeting agent for pancreatic cancer. Nat Commun. 2020;11:4841.
34. Kagechika H, Kawachi E, Hashimoto Y, Shudo K. New type inducers of differentiation of human HL-60 promyelocytic leukemia cells. Terephthalic anilides. Chem Pharm Bull. 1984;32:4209–12.
35. Kagechika H. Novel synthetic retinoids and separation of the pleiotropic retinoidal activities. Curr Med Chem. 2002;9:591–608.
36. Tobita T, Takeshita A, Kitamura K, Ohnishi K, Yanagi M, Hiraoka A, et al. Treatment with a new synthetic retinoid, Am80, of acute promyelocytic leukemia relapsed from complete remission induced by all-trans retinoic acid. Blood. 1997;90:967–73.
37. Hara A, Kobayashi H, Asai N, Saito S, Higuchi T, Kato K, et al. Roles of the mesenchymal stromal/stem cell marker Meflin in cardiac tissue repair and the development of diastolic dysfunction. Circ Res. 2019;125:414–30.
38. Kobayashi H, Gieniec KA, Wright JA, Wang T, Asai N, Mizutani Y, et al. The balance of stromal BMP signaling mediated by GREM1 and ISLR drives colorectal carcinogenesis. Gastroenterology. 2021;160:1224–39.
39. Levental KR, Yu H, Kass L, Lakins JN, Egeblad M, Erler JT, et al. Matrix crosslinking forces tumor progression by enhancing integrin signaling. Cell. 2009;139:891–906.
40. Barker HE, Cox TR, Erler J. The rationale for targeting the LOX family in cancer. Nat Rev Cancer. 2012;12:540–52.
41. Le Calvé B, Griveau A, Vindrieux D, Maréchal R, Wiel C, Svrcek M, et al. Lysyl oxidase family activity promotes resistance of pancreatic ductal adenocarcinoma to chemotherapy by limiting the intratumoral anticancer drug distribution. Oncotarget. 2016;7:32100–12.
42. Yang X, Lin Y, Shi Y, Li B, Liu W, Yin W, et al. FAP promotes immunosuppression by cancer-associated fibroblasts in the tumor microenvironment via STAT3–CCL2 signaling. Cancer Res. 2016;76:4124–35.
43. Puré E, Blomberg R. Pro-tumorigenic roles of fibroblast activation protein in cancer: back to the basics. Oncogene. 2018;37:4343–57.
44. Chen DS, Mellman I. Oncology meets immunology: the cancer-immunity cycle. Immunity. 2013;39:1–10.
45. Gonzalez H, Hagerling C, Werb Z. Roles of the immune system in cancer: from tumor initiation to metastatic progression. Genes Dev. 2018;32:1267–84.
46. Hashimoto Y, Kagechika H, Shudo K. Expression of retinoic acid receptor genes and the ligand-binding selectivity of retinoic acid receptors (RAR's). Biochem Biophys Res Commun. 1990;166:1300–7.
47. Tebben PJ, Singh RJ, Kumar R. Vitamin D-mediated hypercalcemia: mechanisms, diagnosis, and treatment. Endocr Rev. 2016;37:521–47.
48. Klemann C, Raveney BJE, Klemann AK, Ozawa T, von Hörsten S, Shudo K, et al. Synthetic retinoid AM80 inhibits Th17 cells and ameliorates experimental autoimmune encephalomyelitis. Am J Pathol. 2009;174:2234–45.
49. Takaomi S, Kuwano T, Nakao S, Iida S, Ishida T, Komatsu H, et al. Antimyeloma effects of a novel synthetic retinoid Am80 (Tamibarotene) through inhibition of angiogenesis. Leukemia. 2005;19:901–9.
50. Zhang K, Zhang Y, Gu L, Lan M, Liu C, Wang M, et al. Islr regulates canonical Wnt signaling-mediated skeletal muscle regeneration by stabilizing Dishevelled-2 and preventing autophagy. Nat Commun. 2018;9:129.
51. Xu J, Tang Y, Sheng X, Tian Y, Deng M, Du S, et al. Secreted stromal protein ISLR promotes intestinal regeneration by suppressing epithelial Hippo signaling. EMBO J. 2020;39:e103255.

AUTHOR CONTRIBUTIONS
TIi designed and performed the experiments, analyzed the data, and wrote the paper. YM and NE designed and performed the experiments and analyzed the data. SMP and BMB performed SHG analysis. LW performed the mass spectrometric analysis. KKu performed the measurement of intratumoral concentrations of dFdC. KKa, AM, TIs, EO, and HK provided the clinical samples and intellectual input. SI and HH assisted with the analysis of tumor stiffness. SM and YS assisted with histological analysis. HK, YH, MF, and MT directed the project and provided intellectual input. AE directed the project and wrote the paper.

COMPETING INTERESTS
The authors declare no competing interests.

ADDITIONAL INFORMATION
Supplementary information The online version contains supplementary material available at https://doi.org/10.1038/s41388-022-02288-9.

Correspondence and requests for materials should be addressed to Atsushi Enomoto.

Reprints and permission information is available at http://www.nature.com/reprints

Publisher's note Springer Nature remains neutral with regard to jurisdictional claims in published maps and institutional affiliations.